BIOCHEMISTRY
including biophysical chemistry & molecular biology

Article

pubs.acs.org/biochemistry

Rapid Reaction Kinetics of Proline Dehydrogenase in the Multifunctional Proline Utilization A Protein

Michael A. Moxley and Donald F. Becker*

Department of Biochemistry and Redox Biology Center, University of Nebraska—Lincoln, Lincoln, Nebraska 68588, United States

Supporting Information

ABSTRACT: The multifunctional proline utilization A (PutA) flavoenzyme from *Escherichia coli* catalyzes the oxidation of proline to glutamate in two reaction steps using separate proline dehydrogenase (PRODH) and Δ^1-pyrroline-5-carboxylate (P5C) dehydrogenase domains. Here, the kinetic mechanism of PRODH in PutA is studied by stopped-flow kinetics to determine microscopic rate constants for the proline:ubiquinone oxidoreductase mechanism. Stopped-flow data for proline reduction of the flavin cofactor (reductive half-reaction) and oxidation of reduced flavin by CoQ_1 (oxidative half-reaction) were best-fit by a double exponential from which maximum observable rate constants and apparent equilibrium dissociation constants were determined. Flavin semiquinone was not observed in the reductive or oxidative reactions. Microscopic rate constants for steps in the reductive and oxidative half-reactions were obtained by globally fitting the stopped-flow data to a simulated mechanism that includes a chemical step followed by an isomerization event. A microscopic rate constant of 27.5 s^{-1} was determined for proline reduction of the flavin cofactor followed by an isomerization step of 2.2 s^{-1}. The isomerization step is proposed to report on a previously identified flavin-dependent conformational change [Zhang, W. et al. (2007) *Biochemistry 46*, 483−491] that is important for PutA functional switching but is not kinetically relevant to the *in vitro* mechanism. Using CoQ_1, a soluble analogue of ubiquinone, a rate constant of 5.4 s^{-1} was obtained for the oxidation of flavin, thus indicating that this oxidative step is rate-limiting for k_{cat} during catalytic turnover. Steady-state kinetic constants calculated from the microscopic rate constants agree with the experimental k_{cat} and k_{cat}/K_m parameters.

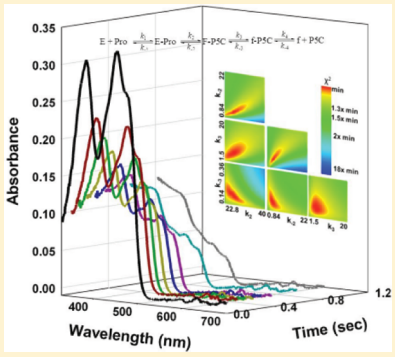

The oxidation of proline to glutamate has significant ramifications in energy and nitrogen metabolism in a variety of organisms.[1] For example, proline oxidative metabolism is important for *Helicobacter pylori* colonization of the gut and in the closely related mouse pathogen *Helicobacter hepaticus*.[2,3] Patients infected with *H. pylori* were reported to have 10-fold higher proline levels than noninfected individuals in the gut, where L-proline is a preferred respiratory substrate of *H. pylori*.[4] In humans, proline serves two roles as a microenvironment energy source and as a pro-apoptotic substrate.[5] Upregulation of proline oxidative metabolism, which occurs in the mitochondrion, leads to increased production of reactive oxygen species and induction of cell death pathways.[6]

Two enzymes, proline dehydrogenase (PRODH) and Δ^1-pyrroline-5-carboxylate dehydrogenase (P5CDH), catalyze the four-electron oxidation of proline to glutamate. In Gram-positive bacteria and eukaryotes, PRODH and P5CDH are separate enzymes, whereas in Gram-negative bacteria such as *H. pylori* and *Escherichia coli*, PRODH and P5CDH are combined into a single polypeptide known as the proline utilization A (PutA) protein.[1,7] Scheme 1 shows the coordinated activities of the PRODH and P5CDH domains in PutA. The PRODH domain of PutA contains a flavin adenine dinucleotide (FAD) cofactor which couples the oxidation of proline (reductive half-reaction) to the reduction of ubiquinone in the membrane (oxidative half-reaction).[8−10] The product of the PRODH reaction, P5C, is next hydrolyzed to γ-glutamate semialdehyde (GSA), which is then oxidized to glutamate in a NAD^+-dependent step catalyzed by the P5CDH domain of PutA.[7,9]

Scheme 1. Oxidation of Proline to Glutamate Catalyzed by the PRODH and P5CDH Domains of PutA

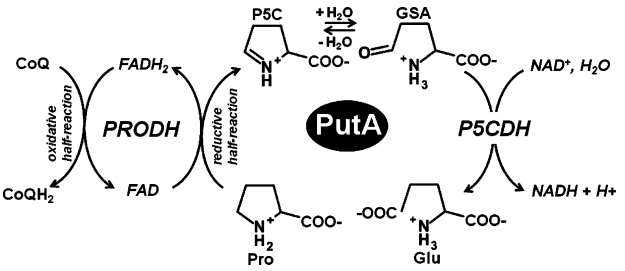

In certain Gram-negative bacteria such as *E. coli* and *Salmonella typhimurium*, PutA also contains a N-terminal ribbon−helix−helix (RHH) DNA binding domain that enables PutA to act as a transcriptional regulatory protein.[11,12] PutA regulates the transcription of the *putA* and *putP* (Na^+/proline transporter) genes according to intracellular proline levels with

Received: October 19, 2011
Revised: December 9, 2011
Published: December 9, 2011

   dx.doi.org/10.1021/bi201603f | *Biochemistry* 2012, 51, 511−520

increases in proline leading to activation of the *put* genes.[13] The mechanism by which PutA regulates *put* gene expression hinges on the redox state of the flavin cofactor and PutA membrane interactions.[14−18] In the oxidized state, cytoplasmic PutA binds to the *put* promoter and represses transcription.[13] When intracellular proline levels increase, the flavin cofactor becomes reduced, causing a dramatic increase in PutA membrane binding affinity.[17] Thus, proline-mediated reduction of the flavin cofactor switches PutA from a transcriptional repressor to a membrane-bound enzyme, which relieves PutA repression of the *put* genes.

PutA from *E. coli* contains 1320 residues with the RHH, PRODH, and P5CDH domains localized at residues 1−52, 261−612, and 650−1130, respectively. X-ray crystal structures have been obtained for the separate RHH/DNA-binding and PRODH domains.[1,13,19] Figure 1A shows the structure of the PutA/PRODH domain from *E. coli*. The PRODH domain has a core $(\beta\alpha)_8$ barrel structure that noncovalently binds the flavin adenine dinucleotide (FAD) cofactor (Figure 1A). The $(\beta\alpha)_8$ barrel core is also found in monfunctional PRODHs from Gram-positive bacteria and is predicted to be similar to the catalytic core of human PRODH.[20] Insights into proline binding were provided by an X-ray crystal structure of the PutA/PRODH domain in complex with the proline analogue, L-tetrahydro-2-furoic acid (L-THFA).[19,21] THFA was observed to bind to the active site with the carboxylate group coordinated by two active site arginine residues (Arg555 and 556) that help position the proline analogue near the *si*-face of flavin (Figure 1B).[21] Thus, far, the only X-ray structure of a full-length PutA is that of the PutA homologue from *Bradyrhizobium japonicum*.[22] PutA from *B. japonicum* is a smaller polypeptide of 999 residues which lacks the RHH/DNA binding domain. The recently solved structure of PutA revealed a 41 Å long cavity linking the PRODH and P5CDH active sites, suggesting that P5C and/or GSA are channeled within PutA.[22]

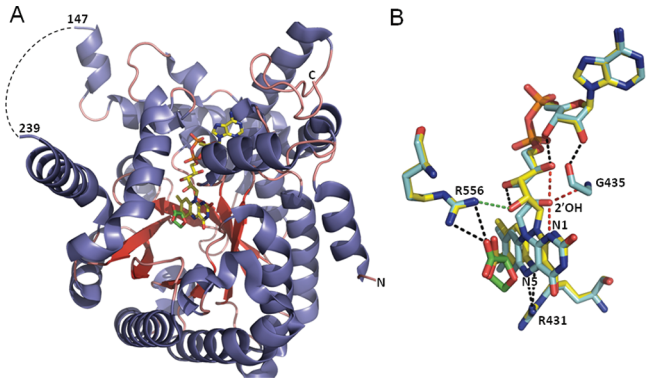

Figure 1. Structure of the PRODH domain and FAD conformations of *E. coli* PutA in oxidized and reduced states. (A) The $(\beta\alpha)_8$ barrel core structure of the PRODH domain is shown, highlighting the locations of the FAD cofactor (yellow) and THFA (green) bound at the *si*-face of FAD (PDB 1tiw). (B) Overlay of the conformational differences in the FAD cofactor between dithionite-reduced (PDB 2fzm) and THFA-bound (PDB 1tiw) PRODH domain structures. THFA-bound structure is colored yellow with THFA highlighted in green. Dithionite-reduced structure is colored teal and has hyposulfite bound in the proline binding site. Black dashed lines represent hydrogen bonds observed in both structures, red dashes are hydrogen bonds unique to the dithionite-reduced structure, and green dashes are hydrogen bonds only observed in the THFA-bound structure. Figures were generated with PyMOL.[39]

The transformation of PutA from a transcriptional repressor to a membrane-associated enzyme, known as functional switching, involves conformational changes that are concomitant with proline reduction of the flavin.[16−18,23,24] A structure of the PutA/PRODH domain reduced with dithionite showed that the FAD adopted a new conformation characterized by a significant "butterfly" bend (22°) of the isoalloxazine ring and rotation of the 2′-OH group of the ribityl chain, resulting in formation of a new hydrogen bond between the 2′-OH and the FAD N(1) atom.[18] Figure 1B highlights the conformational differences of the FAD cofactor between the THFA-bound (i.e., oxidized state) and dithionite-reduced PRODH domain structures. The 2′-OH group of the FAD was subsequently demonstrated to act as a redox-sensitive switch that helps control association of PutA with the membrane.[18] Thus, conformational changes in the FAD upon proline reduction may represent the first step in activating PutA-membrane binding. Another key feature observed in the structures of the PutA/PRODH domain is a hydrogen bond interaction between Arg431 and the FAD N(5) atom. Although no significant conformational changes were observed for Arg431 in the dithionite-reduced structure, Arg431 is proposed to have a critical role in activating PutA membrane binding.[18]

Significant progress has been made toward characterizing key features of PutA such as domain organization and structure, DNA and membrane binding properties, and redox dependent functional switching.[13,18,23,25] A thorough understanding of the mechanisms of PRODH and P5CDH in PutA, however, is still lacking. In particular, rapid reaction kinetics of PutA/PRODH or any related monofunctional PRODH has not yet been performed. Here, we address this gap and provide a comprehensive stopped-flow kinetic analysis of PutA/PRODH. Conventional and global fitting of single turnover data to simulated mechanisms were performed to obtain microscopic rate constants for individual steps in the reductive and oxidative half-reactions of PutA/PRODH from *E. coli*. Steady-state kinetic parameters calculated from the microscopic rate constants showed excellent agreement with previously determined steady-state parameters for the PutA/PRODH reaction.[10] The kinetic data and mechanistic insights reported herein will be of benefit in understanding the mechanisms of PRODH action, intermediate-substrate channeling in PutA, and systems-wide approaches for modeling proline homeostasis in biological systems.[26,27]

EXPERIMENTAL PROCEDURES

Materials. All chemicals and buffers were purchased from Fisher Scientific and Sigma-Aldrich, unless otherwise noted. *E. coli* strains XL-Blue and BL21(DE3) pLysS were purchased from Novagen. DL-P5C was synthesized according to the method of Williams and Frank and stored in 1 M HCl at 4 °C.[28] P5C concentrations were measured by adding *o*-aminobenzaldehyde (*o*-AB) and monitoring the absorbance at 443 nm as mentioned above.[28] PutA was expressed and purified with a N-terminal 6xHis-tag as previously described.[18] After elution of PutA from the anion exchange column (HiTrap Q HP, GE Healthcare) using a 0−1 M NaCl gradient (1 L) in 50 mM Tris (pH 7.5), 0.5 mM EDTA, and 5% glycerol, purified PutA was dialyzed into 50 mM potassium phosphate buffer (pH 7.4) containing 5% glycerol and 50 mM NaCl and stored at −80 °C. The concentration of PutA was determined

spectrophotometrically using a molar extinction coefficient of 12 700 M^{-1} cm^{-1} at 451 nm.[29] All experiments used Nanopure water.

Anaerobic Conditions for Stopped-Flow Experiments. The experiments described herein were conducted under strictly anaerobic conditions to avoid the slow reoxidation of $FADH_2$ by dissolved O_2 which would have distorted the progress curves for the forward (reductive) and reverse (oxidative) half-reactions. Enzyme, substrate, and buffer solutions were degassed, and stopped-flow mixing chambers were washed with deoxygenated buffer for all of the anaerobic experiments described below. Immediately prior to the stopped-flow experiments, PutA in 50 mM potassium phosphate (pH 7.4, 50 mM NaCl and 5% glycerol) and substrate stock solutions were degassed with repeated cycles of vacuum and flushing with oxygen-scrubbed nitrogen. Degassed materials were then brought into an anaerobic glovebox (Belle Technology) to prepare reagents. PutA, buffer, and substrate solutions were transferred to anaerobic syringes under a nitrogen atmosphere in the glovebox. To maintain anaerobic conditions, protocatechuate dioxygenase (PCD) and protocatechuic acid (PCA) were added to the reagents and enzyme solutions at final concentrations of 0.05 U/mL and 100 μM, respectively.[30] Prior to performing the stopped-flow experiments, the stopped-flow mixing chambers were thoroughly washed with anaerobic buffer and incubated overnight with buffer containing PCD/PCA. All stopped-flow experiments were conducted on a Hi-Tech Scientific SF-61DX2 stopped-flow instrument equipped with a photodiode array detector and KinetAsyst software. The temperature of the mixing chamber for all experiments was maintained at 20 °C with a circulating water bath.

Anaerobic Stopped-Flow of the Reductive Half-Reaction with Proline. The reductive half-reaction was examined by rapidly mixing PutA (10 μM after mixing) with varying concentrations of proline (0.025, 0.1, 0.4, 0.8, 1.2, and 1.5 M, after mixing) in 50 mM potassium phosphate (pH 7.4, 50 mM NaCl). The reaction was monitored in the stopped-flow by multiwavelength absorption in the range of 300−700 nm or by single wavelength data collection at 451 nm (A_{451}) where the greatest decrease in flavin absorbance occurs during the reaction. Triplicate traces at 451 nm were fit to eq 1 with KinetAsyst software to obtain observed rate constants (k_{obs1} and k_{obs2}) and the corresponding amplitudes (A_1 and A_2) for the decrease in absorbance at 451 nm. In eq 1, Abs(t) is A_{451} at time t, i is the number of transient phases, A_i and $k_{obs(i)}$ correspond to the amplitude and rate constant for the ith transient phase, respectively, and C is the offset. Observed rate constants were then fit to eq 2 as a function of proline concentration ([S]) to yield the maximum observed rate constant (k_{max}) and the substrate concentration at half-maximal k_{obs} or apparent K_d.

$$\mathrm{Abs}(t) = \sum_{i}^{n} A_i e^{-k_{obs(i)}t} + C \tag{1}$$

$$k_{obs(i)} = \frac{k_{max(i)}[S]}{K_{d(i)}[S]} \tag{2}$$

The reductive half-reaction was also examined by performing a double-mixing experiment. In preparation for the double-mixing experiment, PutA (45 μM) was titrated with proline in the anaerobic chamber with the reduction of the flavin cofactor monitored at 451 nm using a Cary 100 spectrophotometer inside the anaerobic glovebox. Spectra were recorded 5 min after each addition of proline until full reduction of the flavin was obtained. Once fully reduced, the PutA solution was loaded into an anaerobic stopped-flow syringe and attached to the stopped-flow mixing chamber. In the first mixing event, reduced PutA was mixed with 95 μM CoQ_1 and aged for 20 s to allow for full oxidation of the flavin cofactor. In the second mixing event, different concentrations of proline were rapidly mixed with oxidized PutA from the first mixing event in order to reduce PutA a second time. The final concentration of PutA after the second mixing event was 11.25 μM. The reaction of the second mixing event was monitored by multiwavelength absorption in the range 300−700 nm. Single wavelength traces at 451 nm were fitted to eq 1 with KinetAsyst software. The parameters $k_{max(1)}$, $k_{max(2)}$, $K_{d(1)}$, and $K_{d(2)}$ were then obtained by fitting values of $k_{obs(1)}$ and $k_{obs(2)}$ to eq 2, as described above.

Rapid Binding of THFA to PutA. The binding reaction of THFA (neutralized to pH 7.4) to PutA was monitored by rapidly mixing oxidized PutA (31.5 μM after mixing) with different concentrations of L-THFA (2, 4, 8, 16, 32, 100, and 200 mM after mixing) in 50 mM potassium phosphate (pH = 7.4, 50 mM NaCl) at 20 °C. The binding reaction was monitored by multiwavelength absorption (300−700 nm). Kinetic traces of absorbance increases at 476 nm (A_{476}) were collected in triplicate and fit to eq 1 to obtain the amplitude (A) and the observed rate constant (k_{obs}) with Abs(t) corresponding to A_{476} at time t.

Given that pseudo-first-order conditions prevail ([PutA] ≪ [THFA]), the rate constants for the association (k_{on}) and dissociation (k_{off}) steps can be obtained using eq 3, in which the slope is k_{on}, the ordinate intercept is k_{off}, and [THFA] is the variable.

$$k_{obs} = k_{on}[\mathrm{THFA}] + k_{off} \tag{3}$$

The equilibrium dissociation constant (K_d) for the PutA−THFA complex is then obtained by $K_d = k_{off}/k_{on}$. The increase in A_{476} can also be plotted against [THFA] to provide another estimate of K_d, as shown in eq 4, where A_{max} is the maximum amplitude achieved at an extrapolated infinite [THFA].

$$A_{476} = \frac{A_{max}[\mathrm{THFA}]}{K_d + [\mathrm{THFA}]} \tag{4}$$

Oxidative Reaction of Reduced PutA with P5C. Anaerobic oxidized PutA (23.6 μM) was titrated with proline in an anaerobic chamber as described above. PutA was fully reduced with proline at a final concentration of 50 μM. P5C stock solutions (50/50 mixtures of DL-P5C) were neutralized the day of the experiment on ice before being degassed as described above. Reduced PutA was loaded on the anaerobic stopped-flow mixer, shot against varying concentrations of DL-P5C, and followed either by multiwavelength absorption (300−700 nm) or by single wavelength absorption at 451 nm. L-P5C (the active stereoisomer) concentrations ranged from 0.5 to 3.33 mM. Single wavelength traces at 451 nm were best-fit to a single-exponential equation (eq 1) to obtain k_{obs} at different L-P5C concentrations.

Oxidative Half-Reaction with CoQ_1. Oxidized PutA (28 μM) was titrated with proline in an anaerobic chamber as described above. Complete reduction of the flavin was achieved at a final concentration of 50 μM proline. Reduced PutA was

then loaded into an anaerobic stopped-flow syringe and attached to the stopped-flow mixing unit. Proline reduced PutA (14 μM after mixing) was rapidly mixed with varying concentrations of CoQ_1 (0−250 μM, after mixing), and the reaction was monitored by multiwavelength absorption in the range 300−700 nm or by single wavelength data collection at 451 nm. Data were fit to a double exponential (eq 1) with KinetAsyst software. The parameters $k_{max(1)}$, $k_{max(2)}$, $K_{d(1)}$, and $K_{d(2)}$ were then obtained by fitting values of $k_{obs(1)}$ and $k_{obs(2)}$ to eq 2, as described above.

Analysis of the Kinetic Mechanism. In addition to the analytical fitting methods described above, stopped-flow data were analyzed by fitting the data to simulated mechanisms using the KinTek Explorer software (KinTek Corp., Austin, TX).[31−33] The average of at least three kinetic traces obtained at different substrate concentrations was used for the global fitting analysis. Plausible mechanisms deduced from conventional fitting methods were simulated using microscopic rate constants based on analytically fitted parameters, k_{max} and K_d. The association and dissociation rate constants for proline were fitted by using the k_{on} and k_{off} values determined for THFA binding to oxidized PutA as the initial input values and constraining k_{-1}/k_1 to the K_d for proline. For fitting the oxidative half-reaction with CoQ_1, initial values for the association and dissociation rate constants for CoQ_1 (k_5 and k_{-5} in Scheme 2, respectively) were estimated from preliminary

Scheme 2. Mechanisms Used To Simulate the Stopped-Flow Data for the Reductive and Oxidative Half-Reactions by Global Kinetic Explorer[a]

Reductive Half-Reaction

$$E + Pro \underset{k_{-1}}{\overset{k_1}{\rightleftharpoons}} E\text{-}Pro \underset{k_{-2}}{\overset{k_2}{\rightleftharpoons}} F\text{-}P5C \underset{k_{-3}}{\overset{k_3}{\rightleftharpoons}} f\text{-}P5C \underset{k_{-4}}{\overset{k_4}{\rightleftharpoons}} f + P5C$$

Oxidative Half-Reaction

$$f + CoQ \underset{k_{-5}}{\overset{k_5}{\rightleftharpoons}} f\text{-}CoQ \overset{k_6}{\rightleftharpoons} e\text{-}CoQH_2 \overset{k_7}{\rightleftharpoons} E\text{-}CoQH_2$$

[a]E, oxidized PutA conformer 1; F, reduced PutA conformer 1; f, reduced PutA conformer 2; e, oxidized PutA conformer 2.

fits with the best-fit value obtained with k_5 near k_{cat}/K_m and k_{-5}/k_5 fixed by the observed K_d for CoQ_1. Once a near fit of the data was achieved, k_5 and k_{-5} were held fixed by the observed apparent K_d for CoQ_1 and a nonlinear least-squares algorithm was used to refine estimates of the rate constants for the chemical and isomerization steps.[33] An important tool of KinTek Global Explorer is the ability to rigorously determine the confidence intervals for the fitted parameters. The confidence intervals of the parameters were determined for each fitted mechanism and are shown as two-dimensional plots of two fitted parameters and scaled according to the chi squared value (χ^2). These plots are confidence contour plots referred to as FitSpace with rate constants in units of s^{-1} (first order) and mM^{-1} s^{-1} (second order).[32]

RESULTS

Rapid-Reaction Kinetics of the Reductive Half-Reaction. Previously we have shown that PRODH follows a two-site ping-pong steady-state mechanism similar to that observed with other flavin-dependent oxidoreductases.[10] Therefore, we chose to study the proline:ubiquinone oxidoreductase reaction by examining the reductive and oxidative half-reactions separately. The rate constants for individual steps in the reductive half-reaction with proline were determined from the stopped-flow experiments performed under anaerobic conditions. Figure 2A shows the overall absorbance changes in the

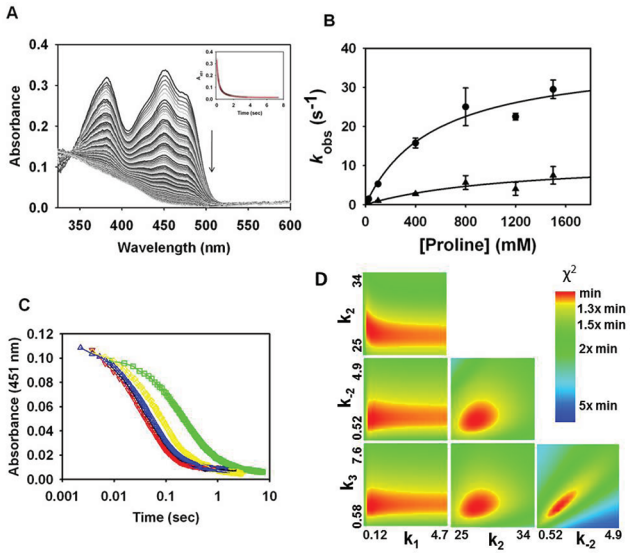

Figure 2. Proline reductive half-reaction. (A) Oxidized PutA (27 μM after mixing) was mixed with 100 mM proline (after mixing) and spectral changes were monitored by stopped-flow multiwavelength absorption using a photodiode array detector. The spectra shown were recorded at 0.025−10 s after mixing. (Inset) Single wavelength trace at 451 nm fit to eq 1. (B) Observed rates constants k_{obs1} and k_{obs2} from the fit to eq 1 were plotted versus proline concentration and fit to eq 2 to yield k_{max} estimates of 38 s^{-1} (k_{obs1}) and 11 s^{-1} (k_{obs2}) and an apparent K_d value of 550 mM. (C) Global fit of the single wavelength traces at 451 nm for the reaction of PutA (10 μM after mixing) with 100 (green), 400 (yellow), 800 (blue), 1200 (black), and 1500 mM (red) proline (concentration after mixing) to the mechanism shown for the reductive half-reaction in Scheme 2. (D) FitSpace contour plots for the global fit of the data. The ratio of k_1 and k_{-1} was fixed by a K_d of 550 mM for proline. Rate constants and best-fit parameters are summarized in Table 1.

reaction of PutA with 100 mM proline and the corresponding decrease in absorbance at 451 nm fit to eq 1 (Figure 2A, inset). FAD semiquinone, the formation of which would have yielded a peak around 380 or 580 nm, was not detected in the reaction. The deconvolution of the observed spectra showed evidence for only the fully reduced and oxidized forms of the flavin cofactor (Supporting Information Figure S1), which is consistent with the proposal that reduction of the flavin proceeds through a hydride transfer.[19] Formation of a carbanion intermediate followed by two rapid single electron transfers, however, is also feasible as short-lived radicals may not be detectable in our experiments. Kinetic traces of the decrease in absorbance at 451 nm at different proline concentrations (0.025−1.5 M) were fitted to a double-exponential equation (eq 1), with relative amplitudes of 80% and 20% for the fast (k_{obs1}) and slow (k_{obs2}) phases, respectively. A plot of k_{obs1} versus proline concentration approached saturation allowing the data to be fit to eq 2, which yielded a k_{max} value of 38 s^{-1} and an apparent K_d = 550 mM proline (Figure 2B, top curve). The slower phase k_{obs2} also showed a saturation dependence on proline concentration with a k_{max} value of 11 s^{-1} (Figure 2B, bottom curve). We did not detect a rapid initial phase with a linear dependence of k_{obs}

dx.doi.org/10.1021/bi201603f | Biochemistry 2012, 51, 511−520

Table 1. Rate Constants Obtained from Analytical and Global Fitting[a]

rate constant	best-fit value	lower bound	upper bound	analytical fitting
		reductive half-reaction		
k_1	506 M^{-1} s^{-1} [b]	0.25 M^{-1} s^{-1}	4.6 × 10^3 M^{-1} s^{-1} [c]	K_d = 550 ± 235 mM
k_{-1}	255 s^{-1} [b]	ND[d]	ND[d]	
k_2	27.5 s^{-1} (27.4)	26 s^{-1} (23)	30 s^{-1} (32)	k_{max} = 38 ± 6 s^{-1}
k_{-2}	1.6 s^{-1} (4.1)	1.1 s^{-1} (1.5)	2.7 s^{-1} (8.4)	
k_3	2.2 s^{-1} (6.3)	1.5 s^{-1} (3.0)	3.7 s^{-1} (11.1)	k_{max} = 11 ± 7 s^{-1}
k_{-3}	(0.19)	(0.16)	(0.25)	
k_4	(95.5)[e]			
k_{-4}	(4.6 × 10^3 M^{-1} s^{-1})[e]			
		oxidative half-reaction		
k_5	21 × 10^3 M^{-1} s^{-1} [f]			K_d = 124 ± 27 μM
k_{-5}	2.9 s^{-1} [f]			
k_6	5.4 s^{-1}	4.4 s^{-1}	7.6 s^{-1}	k_{max} = 7.5 ± 0.7 s^{-1}
k_7	4.7 s^{-1}	3 s^{-1}	18 s^{-1}	k_{max} = 4 ± 2 s^{-1}
		second reductive half-reaction		
k_1'	500 M^{-1} s^{-1} [g]			K_d = 316 ± 60 mM
k_{-1}'	175 s^{-1} [g]			
k_2'	50 s^{-1}	40 s^{-1}	63 s^{-1}	k_{max} = 59 ± 4 s^{-1}
k_{-2}'	6 s^{-1}	4.3 s^{-1}	8.7 s^{-1}	
k_3'	0.42 s^{-1}	0.36 s^{-1}	0.50 s^{-1}	k_{max} = 0.44 ± 0.14 s^{-1}

[a]Values in parentheses are from the global fitting analysis shown in Figure 4. [b]k_1 and k_{-1} were constrained near the K_d of 550 mM for proline. [c]The value given is a result of the default range; however, the upper limit of k_1 is probably unbounded. [d]Not determined because when the ratio of k_{-1}/k_1 is constrained in Global Kinetic Explorer, confidence intervals are only provided for the first parameter (k_1). [e]k_4 was not allowed to be rate determining, and the ratio k_4/k_{-4} was held above 3.3 mM P5C.[10] [f]Were estimated from preliminary fitting and held fixed near the K_d of 124 μM for CoQ_1. [g]k_1' and k_{-1}' were constrained by the K_d of 316 mM for proline.

versus proline concentration, indicating that the proline binding and chemical steps are not observable as well separated kinetic phases in our experiments.

Progress curves for the proline reductive half-reaction (Figure 2C) were fitted to the simulated mechanism shown in Scheme 2 which involves proline binding steps (k_1 and k_{-1}), a reversible step for reduction of the flavin (k_2 and k_{-2}), and an isomerization step following flavin reduction (k_3 and k_{-3}). Product dissociation and association steps (k_4 and k_{-4}) were not included in this part of the analysis. Since the binding of the proline competitive inhibitor, THFA, perturbs the spectrum of the isoalloxazine ring of FAD, we expected that proline binding would lead to a similar spectral perturbation prior to reduction of the flavin. Such a spectral perturbation, however, was not detected suggesting that the proline−PutA complex does not accumulate to a significant amount. Moreover, since we were not able detect the proline binding step, the observed rate constants in Figure 2B were attributed to FAD reduction (k_2) and an isomerization step (k_3). The isomerization step was included in the mechanism because the FAD cofactor has been observed by X-ray crystallography to undergo a significant conformational change upon reduction (Figure 1B). The fitted time traces shown in Figure 2C along with the FitSpace contour plots (Figure 2D) indicate that the rate parameters are well constrained except for k_1, the association rate constant for proline binding. The lack of an upper bound value for k_1 illustrates that the binding step for proline to PutA is not well represented in our data and might occur at a rate much faster than k_{max1} and k_{max2}. Also, in the fitting analysis above, the best-fit was with k_{-3} = 0 (reverse isomerization step), indicating that the isomerization is irreversible or that the rate is too low to be accurately determined by these data alone. The fitted rate constants along with their corresponding confidence intervals are summarized in Table 1.

THFA Binding Kinetics. We performed stopped-flow binding kinetics with THFA as an alternative approach for evaluating substrate binding to PRODH/PutA. THFA is a dead-end competitive inhibitor of proline that mimics proline binding in the active site as shown previously by a structure of THFA bound to the PutA/PRODH domain (Figure 1).[19] The replacement of the secondary amine group of proline with oxygen renders THFA a poor reductant of the FAD cofactor. THFA, however, perturbs the spectrum of the bound FAD cofactor and increases absorbance at 476 nm, thus allowing the kinetics of THFA binding to be conveniently monitored by stopped flow.[34] Varying concentrations of THFA were mixed with oxidized PutA, and changes in absorbance were monitored by multiwavelength absorbance (Figure 3A). The observed rate constant (k_{obs}) for THFA binding was obtained by fitting the increase in absorbance at 476 nm (A_{476}) at each THFA concentration using eq 1. A plot of the k_{obs} values versus THFA concentration was then fitted to eq 3 yielding estimates for k_{on} of 368 M^{-1} s^{-1} and k_{off} of 5 s^{-1}, resulting in a K_d of 13.5 mM (Figure 3B). The single-exponential fit and linear dependence of k_{obs} with THFA concentration indicate a one-step binding mechanism. A K_d for the THFA−PutA complex was also determined from plots of the increase in A_{476} versus THFA concentration, from which a fit of the data to eq 4 yielded a comparable K_d value of 6 mM (Figure 3B, inset).

Kinetic traces at A_{476} acquired at different THFA concentrations were also fitted to a simple binding mechanism with rate constants k_{on} and k_{off} using KinTek Global Explorer (Figure 3C). Fitting the data to a simple binding mechanism yielded k_{on} (417 M^{-1} s^{-1}) and k_{off} (4.2 s^{-1}) values with respective confidence intervals of 375−469 M^{-1} s^{-1} and 3.4−5.1 s^{-1} (Figure 3D). Fitting the data in this manner shows that the rate constants are well constrained and that analytical fitting methods provide a good assessment of the rate constants with

dx.doi.org/10.1021/bi201603f | Biochemistry 2012, 51, 511−520

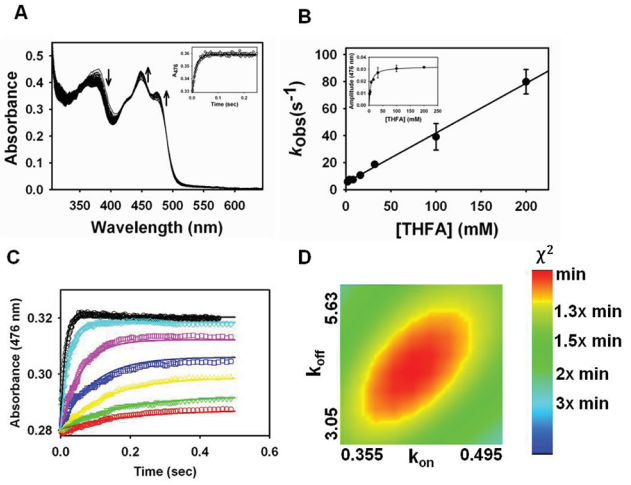

Figure 3. Stopped-flow mixing of THFA with oxidized PutA. (A) Oxidized PutA (31.5 μM after mixing) was mixed with 200 mM THFA (after mixing) and followed by stopped-flow multiwavelength absorption. (Inset) Single wavelength trace at 476 nm fit to a single exponential (eq 1). (B) k_{obs} plotted versus THFA concentration and fit to eq 3 to yield k_{on}= 368 M^{-1} s^{-1} and k_{off} = 5 s^{-1} (K_d = 13.5 mM). (Inset) Amplitude from the fit to eq 3 plotted against the THFA concentration and fit to eq 4 to yield K_d = 6 mM. (C) Global fitting of the single wavelength traces at 476 nm from the rapid mixing of PutA (31.5 μM after mixing) with 2 (red), 4 (green), 8 (yellow), 16 (blue), 32 (pink), 100 (cyan), and 200 mM (black) THFA (after mixing) to a one-step binding mechanism (E + THFA = E−THFA), where k_{on} and k_{off} are the association and dissociation rate constants for THFA binding, respectively. Fitting yielded k_{on}= 417 M^{-1} s^{-1} and k_{off} = 4.2 s^{-1} (K_d = 10.2 mM). (D) FitSpace contour plot of the global fit of the data. Calculated lower and upper bounds are 375−469 M^{-1} s^{-1} and 3.4−5.1 s^{-1} for k_{on} and k_{off}, respectively.

the pseudo-first-order approximation being valid for this case ([PutA] ≪ [THFA]). The k_{on} value obtained for THFA is similar to the best-fit value for k_1 (506 M^{-1} s^{-1}), indicating that a reasonable estimate for the proline association step is obtained from the fitting in Figure 2.

Reversibility of the Reductive Half-Reaction. Global fitting of the data for the reductive half-reaction with KinTek Global Kinetic Explorer indicate that the reductive chemical step is reversible albeit at a relatively slower rate (k_{-2} = 1.6 s^{-1}). To confirm the reversibility of the proline reductive step and attempt to obtain an estimate for the reverse isomerization step (k_{-3}), reduced PutA was rapidly mixed with the product, P5C, and the reaction was monitored by multiwavelength absorption. For these experiments, reduced PutA was made by titrating the enzyme with proline under anaerobic conditions to reduce the flavin cofactor. Figure 4A shows the absorbance changes that occur in the reaction of reduced PutA with P5C. An increase in absorbance at 451 nm occurred with no significant formation of flavin semiquinone during the reaction (Figure S2). The amount of flavin oxidized in the reaction with P5C was estimated to be about 75% of the total flavin. The increase in absorbance at 451 nm was best-fit with a single-exponential equation to give an estimate of an apparent rate constant for the reoxidation step. In the range of P5C concentrations (0.5−3.3 mM) used, only a linear dependence of the observed rate constant on P5C was obtained, suggesting the K_d > 3.3 mM P5C (Figure 4A, inset). We were not able to use higher concentrations of P5C because at neutral pH the second-order rate of P5C polymerization becomes significant >10 mM

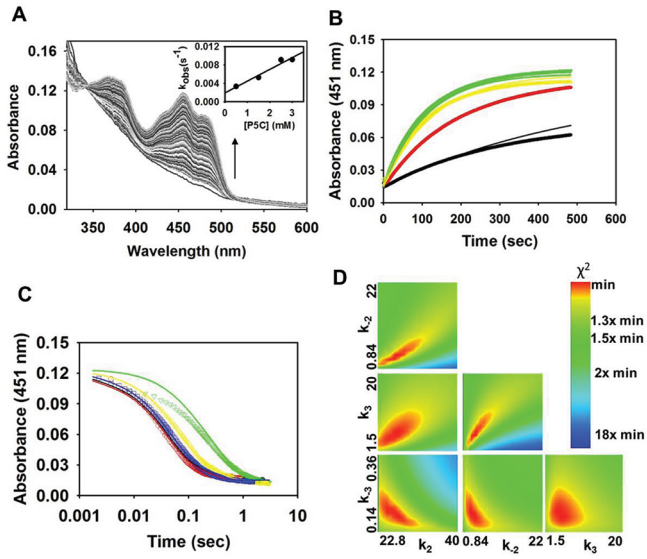

Figure 4. Rapid reaction kinetics of the reverse reaction with P5C. (A) Reduced PutA (11.8 μM after mixing) was mixed with 3.33 mM P5C (after mixing) and followed by stopped-flow multiwavelength absorption. (Inset) Reduced PutA (11.78 μM) was rapidly mixed with 0.5 (black), 1.5 (red), 2.5 (yellow), and 3.3 mM (green) P5C. The observed rate constants from single-exponential fits of the data were plotted against P5C concentration and fit to a line (slope = 2.6 × 10^{-3} and intercept = 1.9 × 10^{-3}). (B, C) Global fitting of the combined data from single wavelength traces at 451 nm for the reverse (B) and forward (C) reactions to the reductive half-reaction shown in Scheme 2. The progress curves in panel C are a replot of the data from Figure 2C. The global fitting in panels B and C also includes amplitudes from multiwavelength data for the proline reductive half-reaction with 100 and 400 mM proline as shown in Figure S4. (D) FitSpace contour plots for the global fitting of the combined data from the reverse and forward reactions. Rate constants and best-fit parameters are summarized in Table 1.

P5C.[35] Thus, only an apparent bimolecular rate constant of 2.6 M^{-1} s^{-1} (k_{max}/K_d) could be estimated from the linear dependence of the reverse reaction with P5C.

Data from the reverse and forward reactions were combined and fitted to the reductive half-reaction mechanism in Scheme 2 using KinTek Global Explorer. Data from the forward reaction included the single wavelength traces shown in Figure 2C and amplitude data from multiwavelength spectra collected at 100 and 400 mM proline. Global fitting of the single wavelength traces for the reverse and forward directions to the reductive half-reaction in Scheme 2 are shown in Figures 4B and 4C, respectively. Global fitting of the multiwavelength amplitude data is shown in Figure S3. FitSpace contour plots in Figure 4D show that values for k_2, k_{-2}, k_3, and k_{-3} are well constrained. The rate constants for the proline (k_1 and k_{-1}) and P5C (k_4 and k_{-4}) binding steps were held fixed in the fitting analysis. The fitted rate constants along with their corresponding confidence intervals are summarized in Table 1. The above analysis of the reverse reaction with P5C confirms the reversibility of the reductive step (k_2 and k_{-2}) and provides an estimate of the microscopic rate constant for the reverse isomerization step (k_{-3}).

Single-Turnover Experiments of the Oxidative Half-Reaction. We next determined rate constants for the oxidative half-reaction by reacting reduced PutA with CoQ_1 under single-turnover conditions. Reduced PutA was generated by titrating with proline (Figure S4) and was rapidly mixed with different

dx.doi.org/10.1021/bi201603f | *Biochemistry* 2012, 51, 511−520

concentrations of CoQ_1. Figure 5A shows the spectra collected after mixing reduced PutA with 60 μM CoQ_1. The absorbance

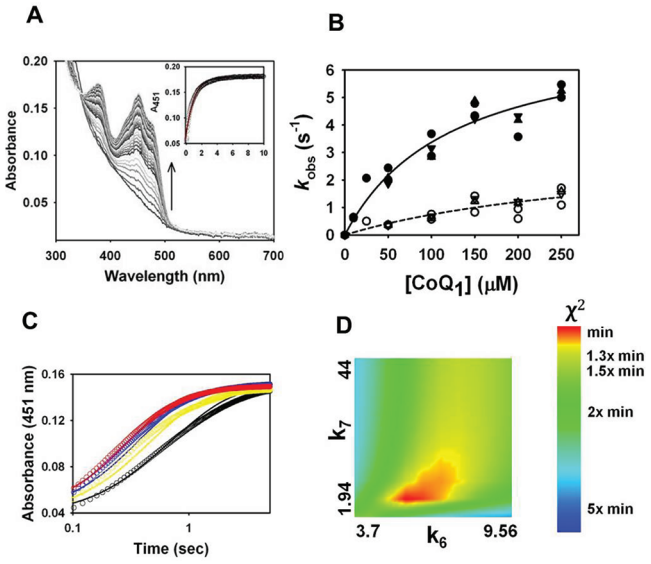

Figure 5. Stopped-flow kinetics of the oxidative half-reaction with CoQ_1. (A) Reduced PutA (15 μM after mixing) was mixed with 60 μM CoQ_1 (after mixing) and monitored by stopped-flow multiwavelength absorption. (Inset) Single wavelength trace at 451 nm fit to eq 1. (B) k_{obs1} and k_{obs2} from fitting to eq 1 were plotted against CoQ_1 concentration and fit to eq 2 yielding a k_{max} of 7.5 s^{-1} and K_d of 124 μM CoQ_1 for k_{obs1} and a k_{max} of 4 s^{-1} for k_{obs2}. (C) Global fit of the single wavelength traces at 451 nm for the reaction of reduced PutA with 100 (black), 150 (yellow), 200 (blue), and 250 μM (red) CoQ_1 (after mixing) fit to the mechanism shown for the oxidative half-reaction in Scheme 2. (D) FitSpace contour plot for the global fitting of the data to the mechanism. Rate constants and best-fit parameters are summarized in Table 1.

at 451 nm increased rapidly with the flavin cofactor becoming fully oxidized by ~5 s (Figure 5A, inset). Flavin semiquinone was not observed in the oxidation of reduced PutA with CoQ_1 as examined by deconvolution of the spectra (Figure S5). The absorbance changes at 451 nm were fitted to a double-exponential equation (eq 1) with two observed rate constants: k_{obs1} (~70% amplitude) and k_{obs2} (~30% amplitude) (Figure 5A, inset). The concentration dependence of $k_{obs(1,2)}$ was performed using 0–250 μM CoQ_1 (Figure 5B). From the best fit of the data, a k_{max} value of 7.5 s^{-1} for the oxidation of reduced FAD and an apparent K_d of 124 μM CoQ_1 were estimated for k_{obs1} while a maximum rate of 4 s^{-1} was estimated for k_{obs2}.

Progress curves of the oxidative half-reaction with CoQ_1 were fitted as shown in Figure 5C to the mechanism shown in Scheme 2 that accounted for two kinetic phases. The mechanism includes the binding of CoQ_1 to reduced PutA (k_5 and k_{-5}), oxidation of the reduced FAD cofactor (k_6), and an isomerization step (k_7). The association (k_5) and dissociation (k_{-5}) rate constants of CoQ_1 with PutA are unknown and were not well constrained in the fit analysis. Therefore, for the global fitting analysis k_5 was best-fit by a value near k_{cat}/K_m and k_{-5}/k_5 was fixed by the apparent K_d for CoQ_1 binding to reduced PutA. The chemical step for the reaction (k_6) was found to be irreversible, as the reverse rate constant was pushed to nearly zero, and therefore this rate constant was fixed at zero for the final fit. Previously, it was shown that CoQ_1H_2 does not reduce PutA, which is consistent with the fitting analysis here.[10] The FitSpace calculations of the fitted rate constants k_6 and k_7 are shown in Figure 5D, demonstrating that they are well constrained. All of the above rate constants are summarized in Table 1.

Second Turnover Stopped-Flow Kinetics. To determine whether the rate constants for proline reduction and the proposed isomerization step were significantly different in subsequent turnovers, the rate constant for flavin reduction in the second turnover was examined by conducting a double mixing experiment with PutA. For these experiments, PutA was first titrated with proline inside an anaerobic chamber to reduce the flavin. Only about a 2-fold excess of proline was needed to fully reduce PutA, resulting in an enzyme that is mostly in the free reduced state. The reduced enzyme was then rapidly mixed with CoQ_1 (95 μM after mixing) to fully reoxidize the flavin in the first mixing event. In the second mixing event, the reoxidized PutA enzyme was reacted with proline to regenerate the reduced enzyme (Figure 6A). The absorbance changes in

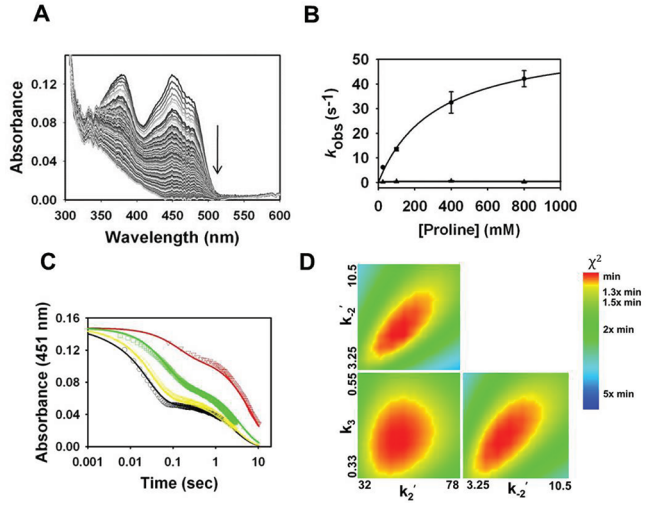

Figure 6. Double-mixing experiment for the proline reductive half-reaction. (A) Reduced PutA (22.5 μM after first mixing) was mixed with 95 μM CoQ_1 (after first mixing) and allowed to age for 20 s. After aging, PutA (11.25 μM after second mixing) was rapidly mixed with 100 mM proline (after mixing) in the second mixing chamber and monitored by stopped-flow multiwavelength absorption. (B) Estimates of k_{obs1} and k_{obs2} from fitting to eq 1 were plotted against different proline concentrations and fit to eq 2, yielding a k_{max} of 59 s^{-1} and K_d of 316 mM proline for k_{obs1} and a k_{max} of 0.44 s^{-1} for k_{obs2}. (C) Single wavelength traces at 451 nm of the data at 25 (red), 100 (green), 400 (yellow), and 800 mM (black) proline (after mixing) were globally fit to the simulated mechanism for the reductive half-reaction in Scheme 2. (D) FitSpace contour plots for the fitted data to the mechanism. Rate constants and best-fit parameters are summarized in Table 1.

the flavin spectrum were similar to that observed in the first reduction event and were fitted to eq 1 (Figure 6A, inset). The observed rate constant (k_{obs1}) for the major amplitude change (70%) at 451 nm displayed saturation kinetics with k_{max} = 59 s^{-1} and apparent K_d = 316 mM proline (Figure 6B). Thus, the observed rate constant for proline reduction of the flavin is slightly higher in the second turnover. The second observed rate constant (k_{obs2}) was significantly slower relative to k_{obs2} in the first turnover experiment and exhibited a much lower dependence on proline concentration, yielding a k_{max} = 0.44 s^{-1}.

dx.doi.org/10.1021/bi201603f | *Biochemistry* 2012, 51, 511–520

Progress curves for the second reductive half-reaction of PutA (Figure 6C) were analyzed by fitting the data to a simulated mechanism identical to the first reductive half-reaction (Scheme 2). Rate constants for proline binding (k_1') and dissociation (k_{-1}') were fixed to similar values determined from the first reduction experiment to maintain an apparent K_d value of 316 mM proline. The best-fit value for the rate constant in the second reduction step (k_2') is increased by 1.8-fold relative to the rate constant of the reduction step in the first turnover (k_2 = 27.5 s^{-1}). The rate constant for the reverse step (k_{-2}') is also faster than the corresponding rate constant in the first turnover (Table 1). The isomerization step (k_3'), however, is about 5-fold slower compared to the corresponding k_3 in the first turnover. The slower isomerization step significantly changes the progress curve as shown in Figure 6C, generating a noticeable biphasic profile relative to the reductive traces observed in the first turnover (Figure 2C). FitSpace calculations shown in Figure 6D demonstrate that k_2', k_{-2}', and k_3' are well constrained by the data. Rate constants for the second reductive half-reaction are summarized in Table 1.

DISCUSSION

The main objective of this study was to obtain microscopic rate constants for the proline:ubiquinone oxidoreductase activity of PutA and derive a more complete kinetic mechanism for PutA/PRODH. A detailed description of the PRODH reaction for PutA can now be assembled by combining steady-state kinetic data and the individual rate constants from the single-turnover experiments conducted here. The steady-state reaction was previously determined to proceed via a two-site ping-pong pathway.[10] Our single-turnover experiments are consistent with a ping-pong mechanism as proline reduction of PutA occurs without CoQ_1. A nonobligatory path involving a ternary complex is also possible; however, only the main two-site ping pong mechanism was used in our analysis.

The kinetic traces for the reductive and oxidative half-reactions were best-fit to a double-exponential equation with the faster rate constant (k_{obs1}) being assigned to the reduction and oxidation of the FAD cofactor and the second observed rate constant (k_{obs2}) assigned to an isomerization step. Assigning the second observed rate constant (k_{obs2}) to an isomerization step seems reasonable because a variety of experimental evidence, including structural analysis of the PRODH domain in different redox states, have demonstrated that PutA undergoes a reversible redox-dependent conformational change.[18,23,25] We excluded the possibility that k_{obs2} is reporting on product release since product release is an obligatory step during steady-state turnover. Previous solvent viscosity studies indicated that diffusion limited steps (e.g., product release) are not significantly rate limiting.[10] Thus, progress curves for the reductive and oxidative half-reactions were globally fitted to a simulated mechanism which included reduction/oxidation steps followed by an isomerization event (Scheme 2). Table 1 summarizes the rate constants determined for the individual steps in the reductive and oxidative half-reactions, including the rate constants for the second reductive half-reaction along with their confidence intervals.

For the reductive half-reaction, the microscopic rate constant determined for proline reduction of the flavin (k_2 = 27.5 s^{-1}) is significantly higher than k_{cat} (5.2 s^{-1}), indicating that flavin reduction is not rate limiting. The microscopic rate constant estimated for oxidation of the flavin cofactor (k_6 = 5.4 s^{-1}) is near the k_{cat} value. Thus, the stopped-flow data indicate that oxidation of the reduced flavin cofactor is the predominant rate-limiting step for the overall reaction with CoQ_1. This is consistent with previous solvent viscosity studies indicating that the overall reaction is most likely limited by a chemical step.[10]

The microscopic rate constants determined for the proposed isomerization step in the reductive (k_3 = 2.2 s^{-1}) and oxidative (k_7 = 4.7 s^{-1}) directions are slightly lower than k_{cat}, indicating that these steps may not be kinetically relevant during multiple turnovers in the steady-state kinetic phase *in vitro*. To see whether the proposed isomerization step was only associated with the first turnover, we performed a double-mixing experiment to examine reduction of the flavin in the second turnover. Surprisingly, the rate of flavin reduction increased by nearly 2-fold (k_2' = 50 s^{-1}), whereas the rate constant for the isomerization step decreased by about 5-fold (k_3' = 0.42 s^{-1}). Thus, the proposed isomerization event appears to be occurring on a much slower time scale in the second turnover and is not kinetically competent for k_{cat}.

The rate constants k_3 and k_7 determined here in the simulated mechanisms (Scheme 2) may be reporting on flavin conformational changes and other protein dynamics involved in PutA functional switching. Figure 1B shows that the conformation of the FAD cofactor differs significantly in the dithionite reduced structure relative to the THFA-bound structure of the PutA/PRODH domain, namely rotation of the 2′-OH group by about 90° to within hydrogen-bonding distance of the N(1) atom of FAD and bending of the isoalloxazine ring.[18] Substitution of normal flavin with 2′-deoxyflavin in PutA has shown that the ribityl 2′-OH is critical for proper redox regulation of PutA membrane binding.[18] A proline-dependent conformational change has also been mapped to a flexible region nearby the PRODH domain (residues 141−262) by limited proteolysis of oxidized and reduced PutA.[23] This same flexible region was also found to undergo a proline-dependent conformational change in a tryptophan fluorescence study of a truncated PutA protein (residues 86−601).[25] Trp211 was identified as the primary marker of proline-induced fluorescence changes with an apparent observed rate constant of about 0.6 s^{-1} determined by stopped-flow fluorescence measurements.[25] The rate constant from the previous fluorescence study is only 3−4-fold slower than k_3 (2.2 s^{-1}) determined here, which further suggests that assigning k_3 to an isomerization step is appropriate.

Unfortunately, we were not able to directly obtain rate constants for proline and CoQ_1 binding to PutA. Substrate binding can sometimes be resolved in pre-steady-state kinetics as a linear trend in k_{obs} versus substrate concentration.[36] However, concomitant changes in the absorbance of the FAD cofactor occur with both substrates upon binding to PutA, making it difficult to observe binding steps. Thus, the association and dissociation rate constants for proline and CoQ_1 are only best estimates from the global fitting analysis. The estimate for the association rate of proline binding agrees well with that obtained with THFA. It is apparent, however, that the best-fit estimate of the dissociation rate constant for proline (255 s^{-1}) is much faster than THFA (5 s^{-1}), which explains why the K_d value for proline is 100-fold higher than for THFA. The one-step binding mechanism observed for THFA also confirms that the isomerization step included in the reductive half-reaction occurs after reduction of the flavin cofactor.

A steady-state mechanism for PutA that is consistent with a two-site ping-pong mechanism and the single-turnover data above was derived for the proline:ubiquinone oxidoreductase reaction catalyzed by PutA (see Supporting Information). The derivation includes the proposed isomerization step; however, this step cancels when the conformational change leads to an enzyme state that has identical catalytic properties. In other words, the steady-state kinetic parameters have identical definitions in terms of microscopic rate constants with or without the isomerization step. Thus, the proposed isomerization step is effectively off the kinetic path so that it does not limit the steady-state turnover rate *in vitro*. This is illustrated in Scheme S1 of the Supporting Information. After the reduced enzyme product complex (F−P5C) is generated in the reductive half-reaction, it can become rapidly oxidized by CoQ before any isomerization step occurs. In this scenario, the isomerization of F to f or e to E does not occur on the kinetic path and is not required for catalysis. The kinetic paths utilizing the E/F and e/f forms can function independently with isomerization steps not affecting catalysis. In the case of PutA, E and F would represent the cytoplasmic conformers, whereas e and f are the membrane bound forms of PutA. Thus, the conformational change is not required for PutA/PRODH catalysis *in vitro* using soluble CoQ_1 analogues; however, a conformational change is required *in vivo* for PutA to switch from a transcriptional repressor to a membrane-bound enzyme and access native CoQ substrate.

To validate the overall mechanism, the microscopic rate constants in Table 1 were used to calculate steady-state kinetic parameters. The parameters calculated from the best-fit microscopic rate constants are reported in Table 2 and are in good agreement with the experimental steady-state parameters, further supporting the proposed mechanism.

Table 2. Michaelis Constants Calculated from Microscopic Rate Constants for Proline and CoQ_1

parameter	experimental[a]	calculated[b]
k_{cat}	5.2 ± 0.3 s^{-1}	4.9 ± 0.5 s^{-1}
$K_{mA(pro)}$	42 ± 4 mM	34 ± 2 mM
$K_{mB(CoQ)}$	112 ± 11 μM	124 ± 8 μM

[a] k_{cat}, K_{mA}, and K_{mB} values were previously determined by fitting steady-state kinetic data with the ping-pong equation.[10] [b] Parameters were calculated from microscopic rate constants obtained from the second turnover reductive half-reaction.

The mechanism presented here for PutA proline:ubiquinone oxidoreductase activity is with CoQ_1, and the data indicate that the oxidative step ($FADH_2$ oxidation by CoQ_1) is rate-determining. In the physiological setting, however, PutA must access CoQ in the cytoplasmic membrane. Previously, it was observed that k_{cat} decreases to 0.6 s^{-1} using saturating amounts of *E. coli* membrane inverted vesicles as the electron acceptor.[10] The lower k_{cat} value could be due to the isomerization step being required for turnover with membrane vesicles. Because a conformational change is required for PutA membrane binding, it is reasonable that the isomerization step observed by stopped flow may be the rate-limiting step *in vivo*. However, the k_{cat} values are also lower relative to CoQ_1 using CoQ_2 (1 s^{-1}) and CoQ_4 (0.2 s^{-1}) as alternative substrates.[10] Thus, the decrease in k_{cat} with membrane vesicles could also be due to a slower rate constant for the oxidative step with different CoQ substrates such as CoQ_8 assumed to be in the membrane vesicles. It is also possible that an additional membrane binding step would affect the overall reaction rate which would be obligatory for membrane vesicles and CoQ_4, which requires detergent in the assays 2-fold above the critical micelle concentration (468 μM, Triton X-100), creating a membrane-like environment. A surface dilution kinetic model that is based on the idea that the enzyme binds the micelle/membrane first before it can access the substrate, creating an *in vivo* like environment, has been implemented for peripheral membrane binding proteins.[37,38] A future study using a surface dilution kinetic strategy would be useful with PutA.

In summary, we have determined the microscopic rate constants for the proline:ubiquinone oxidoreductase activity of PutA and show that the microscopic rates are consistent with a two-site ping-pong mechanism for the overall reaction. The rate-limiting step for k_{cat} during catalytic turnover with CoQ_1 can be attributed to the oxidative half-reaction since it is slowest forward obligatory step. In the presence of a membrane, the situation is less clear and will require additional experiments to resolve whether the oxidation of the flavin, isomerization leading to membrane binding, or possibly both steps are rate limiting in the overall reaction. The proposed isomerization step in both the reductive and oxidative directions is consistent with a redox-dependent reversible conformational change in PutA as reported previously.[23] Our results also provide a solid foundation for future studies of substrate channeling kinetics in PutA enzymes.

■ ASSOCIATED CONTENT

Supporting Information

Derivation of the rate equations for the two-site ping-pong rapid equilibrium mechanism for PutA, Scheme S1, and Figures S1−S5. This material is available free of charge via the Internet at http://pubs.acs.org.

■ AUTHOR INFORMATION

Corresponding Author

* E-mail: dbecker3@unl.edu. Phone: 402-472-9652. Fax: 402-472-472-7842.

Funding

This research was supported by NIH GM061068 and is a contribution of the University of Nebraska Agricultural Research Division, supported in part by funds provided through the Hatch Act. This publication was also made possible by NIH Grant P20 RR-017675-02 from the National Center for Research Resources.

■ ACKNOWLEDGMENTS

We thank Dr. Kenneth Johnson for assistance with KinTek Explorer and Dr. Javier Seravalli for his valuable input into this study.

■ ABBREVIATIONS

PutA, proline utilization A; FAD, flavin adenine dinucleotide; *put*, proline utilization; NAD^+, nicotinamide adenine dinucleotide; PRODH, proline dehydrogenase; P5CDH, Δ^1-pyrroline-5-carboxylate dehydrogenase; P5C, Δ^1-pyrroline-5-carboxylate; THFA, tetrahydro-2-furoic acid; EDTA, ethylenediaminetetraacetic acid; GSA, γ-glutamic acid semialdehyde; PCD, protocatechuate dioxygenase; PCA, protocatechuic acid; CoQ, ubiquinone; *o*-AB, *o*-aminobenzaldehyde; RHH, ribbon−helix−helix.

REFERENCES

(1) Tanner, J. J. (2008) Structural biology of proline catabolism. *Amino Acids 35*, 719−730.

(2) Nakajima, K., Natsu, S., Mizote, T., Nagata, Y., Aoyania, K., Fukuda, Y., and Nagata, K. (2008) Possible involvement of *putA* gene in *Helicobacter pylori* colonization in the stomach and motility. *Biomed. Res. 29*, 9−18.

(3) Krishnan, N., Doster, A. R., Duhamel, G. E., and Becker, D. F. (2008) Characterization of a *Helicobacter hepaticus putA* mutant strain in host colonization and oxidative stress. *Infect. Immun. 76*, 3037−3044.

(4) Nagata, K., Nagata, Y., Sato, T., Fujino, M. A., Nakajima, K., and Tamura, T. (2003) L-Serine, D- and L-proline and alanine as respiratory substrates of *Helicobacter pylori*: correlation between in vitro and in vivo amino acid levels. *Microbiology 149*, 2023−2030.

(5) Phang, J. M., Pandhare, J., and Liu, Y. (2008) The metabolism of proline as microenvironmental stress substrate. *J. Nutr. 138*, 2008S−2015S.

(6) Liu, Y., Borchert, G. L., Surazynski, A., Hu, C. A., and Phang, J. M. (2006) Proline oxidase activates both intrinsic and extrinsic pathways for apoptosis: the role of ROS/superoxides, NFAT and MEK/ERK signaling. *Oncogene 25*, 5640−5647.

(7) Menzel, R., and Roth, J. (1981) Enzymatic properties of the purified *putA* protein from *Salmonella typhimurium*. *J. Biol. Chem. 256*, 9762−9766.

(8) Abrahamson, J. L. A., Baker, L. G., Stephenson, J. T., and Wood, J. M. (1983) Proline dehydrogenase from *Escherichia* K12, properties of the membrane-associated enzyme. *Eur. J. Biochem. 134*, 77−82.

(9) Brown, E., and Wood, J. M. (1992) Redesigned purification yields a fully functional PutA protein dimer from *Escherichia coli*. *J. Biol. Chem. 267*, 13086−13092.

(10) Moxley, M. A., Tanner, J. J., and Becker, D. F. (2011) Steady-state kinetic mechanism of the proline:ubiquinone oxidoreductase activity of Proline Utilization A (PutA) from *Escherichia coli*. *Arch. Biochem. Biophys. 516*, 113−120.

(11) Gu, D., Zhou, Y., Kallhoff, V., Baban, B., Tanner, J. J., and Becker, D. F. (2004) Identification and characterization of the DNA-binding domain of the multifunctional PutA flavoenzyme. *J. Biol. Chem. 279*, 31171−31176.

(12) Halouska, S., Zhou, Y., Becker, D. F., and Powers, R. (2008) Solution structure of the *Pseudomonas putida* protein PpPutA45 and its DNA complex. *Proteins 75*, 12−27.

(13) Zhou, Y., Larson, J. D., Bottoms, C. A., Arturo, E. C., Henzl, M. T., Jenkins, J. L., Nix, J. C., Becker, D. F., and Tanner, J. J. (2008) Structural basis of the transcriptional regulation of the proline utilization regulon by multifunctional PutA. *J. Mol. Biol. 381*, 174−188.

(14) Wood, J. (1987) Membrane association of proline dehydrogenase in *Escherichia coli* is redox dependent. *Proc. Natl. Acad. Sci. U. S. A. 84*, 373−377.

(15) Surber, M. W., and Maloy, S. (1999) Regulation of flavin dehydrogenase compartmentalization: Requirements for PutA-membrane association in *Salmonella typhimurium*. *Biochim. Biophys. Acta 1421*, 5−18.

(16) Brown, E. D., and Wood, J. M. (1993) Conformational change and membrane association of the PutA protein are coincident with reduction of its FAD cofactor by proline. *J. Biol. Chem. 268*, 8972−8979.

(17) Zhang, W., Zhou, Y., and Becker, D. F. (2004) Regulation of PutA-membrane associations by flavin adenine dinucleotide reduction. *Biochemistry 43*, 13165−13174.

(18) Zhang, W., Zhang, M., Zhu, W., Zhou, Y., Wanduragala, S., Rewinkel, D., Tanner, J. J., and Becker, D. F. (2007) Redox-induced changes in flavin structure and roles of flavin N(5) and the ribityl 2′-OH group in regulating PutA-membrane binding. *Biochemistry 46*, 483−491.

(19) Lee, Y. H., Nadaraia, S., Gu, D., Becker, D. F., and Tanner, J. J. (2003) Structure of the proline dehydrogenase domain of the multifunctional PutA flavoprotein. *Nat. Struct. Biol. 10*, 109−114.

(20) White, T. A., Krishnan, N., Becker, D. F., and Tanner, J. J. (2007) Structure and kinetics of monofunctional proline dehydrogenase from *Thermus thermophilus*. *J. Biol. Chem. 282*, 14316−14327.

(21) Zhang, M., White, T. A., Schuermann, J. P., Baban, B. A., Becker, D. F., and Tanner, J. J. (2004) Structures of the *Escherichia coli* PutA proline dehydrogenase domain in complex with competitive inhibitors. *Biochemistry 43*, 12539−12548.

(22) Srivastava, D., Schuermann, J. P., White, T. A., Krishnan, N., Sanyal, N., Hura, G. L., Tan, A., Henzl, M. T., Becker, D. F., and Tanner, J. J. (2010) Crystal structure of the bifunctional proline utilization A flavoenzyme from *Bradyrhizobium japonicum*. *Proc. Natl. Acad. Sci. U. S. A. 107*, 2878−2883.

(23) Zhu, W., and Becker, D. F. (2003) Flavin redox state triggers conformational changes in the PutA protein from *Escherichia coli*. *Biochemistry 42*, 5469−5477.

(24) Becker, D. F., Zhu, W., and Moxley, M. A. (2011) Flavin redox switching of protein functions. *Antioxid. Redox Signal. 14*, 1079−1091.

(25) Zhu, W., and Becker, D. F. (2005) Exploring the proline-dependent conformational change in the multifunctional PutA flavoprotein by tryptophan fluorescence spectroscopy. *Biochemistry 44*, 12297−12306.

(26) Sauer, U., Heinemann, M., and Zamboni, N. (2007) Genetics. Getting closer to the whole picture. *Science 316*, 550−551.

(27) Beard, D. A., and Qian, H. (2008) *Chemical Biophysics: Quantitative Analysis of Cellular Systems*, Cambridge University Press, Cambridge, NY.

(28) Williams, I., and Frank, L. (1975) Improved chemical synthesis and enzymatic assay of delta-1-pyrroline-5-carboxylic acid. *Anal. Biochem. 64*, 85−97.

(29) Becker, D. F., and Thomas, E. A. (2001) Redox properties of the PutA protein from *Escherichia coli* and the influence of the flavin redox state on PutA-DNA interactions. *Biochemistry 40*, 4714−4722.

(30) Patil, P. V., and Ballou, D. P. (2000) The use of protocatechuate dioxygenase for maintaining anaerobic conditions in biochemical experiments. *Anal. Biochem. 286*, 187−192.

(31) Johnson, K. A., Simpson, Z. B., and Blom, T. (2009) Global kinetic explorer: a new computer program for dynamic simulation and fitting of kinetic data. *Anal. Biochem. 387*, 20−29.

(32) Johnson, K. A., Simpson, Z. B., and Blom, T. (2009) FitSpace explorer: an algorithm to evaluate multidimensional parameter space in fitting kinetic data. *Anal. Biochem. 387*, 30−41.

(33) Johnson, K. A. (2009) Fitting enzyme kinetic data with KinTek Global Kinetic Explorer. *Methods Enzymol. 467*, 601−626.

(34) Zhu, W., Gincherman, Y., Docherty, P., Spilling, C. D., and Becker, D. F. (2002) Effects of proline analog binding on the spectroscopic and redox properties of PutA. *Arch. Biochem. Biophys. 408*, 131−136.

(35) Mezl, V. A., and Knox, W. E. (1976) Properties and analysis of a stable derivative of pyrroline-5-carboxylic acid for use in metabolic studies. *Anal. Biochem. 74*, 430−440.

(36) Johnson, K. A. (1992) in *The Enzymes* (Sigman, D. S., Ed.) pp 1−60, Academic Press, New York.

(37) Malmquist, N. A., Baldwin, J., and Phillips, M. A. (2007) Detergent-dependent kinetics of truncated Plasmodium falciparum dihydroorotate dehydrogenase. *J. Biol. Chem. 282*, 12678−12686.

(38) Carman, G. M., Deems, R. A., and Dennis, E. A. (1995) Lipid signaling enzymes and surface dilution kinetics. *J. Biol. Chem. 270*, 18711−18714.

(39) Schrodinger, L. L. C. (2010) The PyMOL Molecular Graphics System, Version 0.99.